Strength and Deformational Characteristics of Orthogonally Reinforced Concrete Containment Models Subjected to Lateral Forces

Y. Aoyagi
Central Research Institute of Electric Power Industry, 1646, Abiko, Abiko-shi, Chiba, Japan

S. Ohmori
Kajima Institute of Construction Technology, 2-19-1 Tobitakuy, Chofu-shi, Tokyo 182, Japan

K. Yamada
Technical Research Institute of Maeda Construction Company, 1-39-16, Asahicho, Nerima-ku, Tokyo, Japan

SUMMARY

The purposes of this study are to clarify the strength and deformational behaviors of orthogonally reinforced concrete containment vessels (RCCV) subject to lateral forces with or wihtout internal pressures, and to investigate stress-strain relationships as well as the load causing yield in steel of cracked reinforced concrete shell elements.

One/ twenty fifth scaled cylindrical models, internal diameter, internal height and wall thickness of which were 154cm, 160cm and 6cm, respectively, and in which the reinforcement ratios (1.8∿3.0%) and the internal pressures (0∿4.5kg/cm^2) were varied, were made and loaded up to failure by reciprocated cyclic horizontal forces. The model was reinforced with the same amount of ϕ6mm deformed bars in two layers in each direction. Test results of six specimens are presented and discussed in this paper, including four models previously reported.

In addition to the cylindrical models, five orthogonally reinforced concrete flat plate specimens, the dimension in plan, the thickness and the reinforcement ratios of which were 150×150cm, 10cm and 1.2%, respectively, were made and subjected to in-plane uniaxial or biaxial forces. The parameters changed in the experiment were the angle between the directions of reinforcement and principal stress and the ratios of two principal stresses.

Followings are the main conclusions obtained within the limit of experiment.

(1) Shearing stresses causing initial yield of steel in the web regions of cylindrical models can reasonably be predicted up to 1.5% in terms of the shear reinforcement ratios(P_w). When P_w exceeds this limit, checks should be made against brittle shear-compression failure.

(2) From the viewpoint of practical design averaged shear stresses calculated by the above equation for both directions of reinforcements may be regarded as a shear stress corresponding to the load giving rise to yield in the direction other than that for the initial yielding.

(3) As substantial deviation of the direction of principal stress with respect to that of steel leads to much increased deformation of shell elements, due account should be paid to the deformational behaviors even when strength requirement is met by using orthogonal arrangement of bars.

(4) In defining load-horizontal-deformation relationships to be applied to the analyses of dynamic responses for RCCV special caution should be excercised to the shear deformations, because they were found to constitute 40∿60% of total horizontal deformations at the top of the cylindrical models in post-diagonal-cracked stage.

1. Introduction

The strength and deformational behaviors of reinforced concrete shell elements which are subjected to in-plane membrance stresses combined with shear and those of reinforced concrete containment vessels (RCCV) models under the action of lateral forces with or without internal pressure were reported in the previous reports [1], [2]. Those studies provided fundamental data for the design of RCCV against earthquake forces, including the conclusions that shear yield capacities of RCCV may reasonably be predicted in terms of effective shear reinforcement ratios when the shear stress remains under the limiting value, and that modified Baumann's theory or Leitz's theory may be applicable to estimade the stresses in reinforcements as well as deformations of RC shell elements.

In the mean time, supplementary tests had been conducted on shell elements as well as on cylindrical models in order to fill up the gap left in the previous tests. The main purposes of the supplementary experiments were to confirm the validity of the conclusions in broader range of reinforcement ratios and to deduce an appropriate estimation method of stresses not only in the weaker but also in the stronger directions of orthogonal bar arrangement systems.

2. Outlines of Experiments

2.1 RC Plate Elements

Dimensions of the plate specimens and the method of load application are the same as previously reproted except for the reinforcement ratio of 1.183% as against 0.763% for the previous one. The reinforcement ratio was selected so as to bring the value as close as possible to that in prototype structures and to secure ample load increase from cracking in concrete up to yielding in steel.

The main data of the supplementary test, which consisted of 6 specimens are summarized in Table-1. Deviation angle of reinforcements with respect to the principal tensile force was fixed at 22.5° with the exceptions of No.22 and No.26 specimens. All the specimens were reinforced equally in amount in both directions but for the specimen No.24, in which the reinforcement ratio in the weaker direction (y-direction) was halved as that in the stronger direction (x-direction). All the specimens except for No.27 were tensioned uniaxially. Two layers of ϕ10mm deformed bars with a spacing of 15cm were arranged to guarantee the prescribed reinforcement ratio. Typical cracking pattern of plate specimen after failure can be seen in Fig.-1.

2.2 Hollow Cylindrical RCCV Models

Two orthogonally reinforced concrete models were added to the four models previously tested. One model, which was reinforced with 1.8% reinforcement in both cicumferential and vertical directions, was subjected to reciprocated lateral forces in the absence of internal pressure. The other one, which had the reinforcement ratio of 3.0%, was also laterally loaded up to failure with the presence of internal pressure of 3.0kg/cm^2. The properties and the test results of the models are listed in Table-2. The models were constructed after the pattern of RCCV for BWR Mark III with a scale of about 1/25. The middle plane diameter as well as the height of the cylindrical wall were 160cm, and the wall with a thickness of 6cm was reinforced orthogonallv with double layers of ϕ6mm deformed bars in each direction.

Details of the load application procedures are deleted here because they are essentially the same as thos previously reported [2].

The model C-1.8-0.0 failed in a shear-compression like fashion in the region of mid-height of wall immediately after yielding in reinforcements at the load of 78.8tons. For the case of the model C-3.0-3.0, yieldings of the reinforcing bars of both directions were observed in the web region at the load of 99 tons and ultimately failed explosively in shear in the lower web part of wall at the load of 127.7 tons.

3. Stress-Strain Characteristics of RC Shell Elements Subjected to In-plane Forces

3.1 Basic Theory

According to Baumann [3] stresses in reinforcements as well as compressive forces in concrete struts can be estimated based on the equilibrium of forces acting on a preassumed crack surface by the eq (1) in reference [1]. (see also Fig-2 in reference [1]). Because of the indeterminate nature of the equilibrium equation the angle of the crack with respect to y reinforcement as well as shear forces occuring along the crack must be determined based either on theoretical compatibility conditions for deformations or on experimentally obtained evidences. A statistical analysis of the crack angles ϕ up to yielding in x reinforcement obtained through the tests of RC shell elements showed that main influencing factors on ϕ are the deviation angle of bars α and the ratio k of algebraic magnitudes of the applied principal forces in both directions. That is, it was found to be practically justifiable to assume that in the domain of uniaxial tension to compression-tension ($k \leqq 0$) ϕ may be assumed equal to α, while at the point of equal biaxial tensions (k=1) ϕ may be fixed at an angle of 45° regardless of the values of α. In the intermediate region ($0<k<1$) ϕ can be linearly interpolated in terms of k as illustrated in Fig. 2.

Unknown shear force H is calculated by the following equation developed originally by Baumann.

$$H = N\{\lambda\cot\phi[\sin^2\alpha(1 + \cot\alpha\cot\phi) + k\cos^2\alpha(1 - \tan\alpha\cot\phi)] - \tan\phi[\cos^2\alpha(1+\tan\alpha\tan\phi) + k\sin^2\alpha(1 - \cot\alpha\tan\phi)] + \nu_{\pm}2\cot 2\phi(1 - k)\sin 2\alpha/\sin 2\phi\}:\{\tan^2\phi + \lambda\cot^2\phi + \nu_{\pm}4\cot^2(2\phi) + \chi\} \quad (1)$$

Main notations appearing in the above equation are defined in Fig. 2 in reference [1] and ν denote Px/Py and EsPx/Ec, respectively. Px, Py, Es and Ec are reinforcement ratios in x and y directions, and Young's modulus of steel and concrete, respectively. χ is defined as ExPx/Ev, which is related to average shear rigidity Ev measured across cracks. Referring to the results of the push-off tests obtained by the authors on precracked reinforced concrete blocks, Ev could be approximately expressed as a function of crack widths as follows:

$$Ev = \frac{540}{Wm} \quad (kg/cm^2) \quad (2)$$

where, Wm: average crack width in mm.

The crack width Wm is, on the other hand, a function of average strains of shell element perpendicular to the direction of cracks. Average crack width Wm is calcualted by multiplying the average strain ε_ϕ by the average crack spacing a_m. ε_ϕ can be predicted using the equations (1) and (2) in reference [1]. Trial fitting of the experimental data to the estimated led to a modification of eq. (3) in reference [1]. In the modified

equation the power of the second term of CEB formula was changed to 3 in lieu of the original 2. This may explain the fact that in a plate element subject to membrane forces degradation of bond between concrete and steel proceeds more rapidly than in ordinary RC beams or slabs. The resulting equations adopted are as follows. (see the notations in reference [1])

$$\varepsilon_{xm} = \varepsilon_x[1 - (\frac{\sigma_{x,cr}}{\sigma_x})^3] \quad , \quad \varepsilon_{ym} = \varepsilon_y[1 - (\frac{\sigma_{y,cr}}{\sigma_y})^3] \tag{3}$$

The crack spacing can be obtained by applying such formula as provided in CEB Code. From the eq (1) in reference [1], the following equation is derived, which relates the sum of the forces in reinforcements in both directions to shear forces along the crack H.

$$Z_x + Z_y = (N_1 + N_2) + (N_1 - N_2) \sin\alpha\cos\alpha(\tan\phi + \cot\phi) + H(\tan\phi - \cot\phi) \tag{4}$$

As the crack angle ϕ is automatically given by the deviation angle α and external stress ratios k, the problem is reduced to the determination of only H. The computation can be conducted by an iterative process depicted in Fig.-3. Once the value of H is fixed, all the other values required, including stresses in reinforcements, axial deformations, crack widths and shear deformations across a crack can be computed by applying the similar procedures as those in reference [1].

3.2 Comparison of Analytical Results with Experimental Data

3.2.1 Average Strains in Reinforcements

In Fig.-4 steel strain changes of the NO23 specimen averaged over a length of spanning several cracks with increasing loads are compared in both x and y directions with those calculated by the methods proposed by Leitz, Baumann and the authors. While the calculated strains in the x direction are practically identical among the three methods and provide a good fit to the measured, in the y direction the agreement seems distinctively better for the author's than the otehr two methods. Substantially the same results were obtained for the cases of the unbalanced reinforced specimen (NO24) subjected to uniaxial tension as well as the equally reinforced specimen (NO27) subjected to biaxial tension.

3.2.2 Yielding Loads in the x (weaker) Direction

The ratios of calculated and measured loads causing yield in the x bars are plotted in Fig.-5 in terms of principal stress ratios of k. The plotted data include the test results previously reproted. It can be seen that although there are no distinct differences between the accuracies of preditiction obtained by Bauman and authors over the range of k investigated, Leitz's theory has a tendency to underestimate the test results in the compression-tension region.

3.2.3 Deformations and Shear Slip

Fig.-6 shows comparisons of measured average post-cracked deformations of the principal tensile force N_1 with the results computed by the authors for the cases of α = 0, 22.5° and 45°. The deformations, which remarkably become larger with increase in deviation angle α, can also be predicted fairly well by the analytical procedures proposed.

In Fig.-7 relative shear slips along a crack are plotted against the applied principal forces N_1, together with the calculated values based on the data of push-off tests (eq (1))

as well as derived by the theoretically obtained strains in reinforcements (eq (2) in reference [1]). It seems that the two kinds of estimations give similar results with a good fit to the experimental values, which may support the validity of the assumption adopted for the evaluation of shear rigidities.

3.3 Prediction of Loads causing Yield in the y (stronger) Reinforcement

It is not unusual that two way reinforced concrete plate elements subjected to in-plane forces sustain some additional load after yielding in the x (weaker) reinforcement when shear compression failures can be avoided. This is generally the case with the RCCV, which is reinforced equally in both directions and is loaded by combined action of internal pressure and lateral forces. Also, the above upper yielding load is closely connected to ultimate shear strength of a RCCV, and, consequently, is considered to be an important reference point in defining a load-horizontal deformation relationship of the structure.

From the above view point the authors derived a formula to predict the load causing yield in the y reinforcement based on the aforementioned theory. In this analysis an assumption was made that after the x reinforcement has yielded, increment of load is to be resisted only by the stress increase in the y reinforcement and the shear to be transferred across the crack H. The crack angle ϕ was assumed to retain its original value in the pre-yielding stage. The resulting formula to calculate the increment of load required to give rise to yielding in the y reinforcement is as follows.

$$\Delta N_1 = \frac{\Delta Z_y \sin 2\phi}{(1 + k)\sin 2\phi + (1 - k)\sin 2\alpha} \qquad (4)$$

where ΔN_1: increase of the principal force N_1 per unit width of the plate element after yielding in x reinforcement.

$$\Delta Z_y = Z_y^{Yield,y} - Z_y^{Yield,x}$$

$Z_y^{Yield,y}$: yield capacity per unit width in the y direction

$Z_y^{Yield,x}$: the y directional force per unit width when the x reinforcement just yielded.

The ratios between measured and calculated values of loads causing yield in the y direction are plotted in terms of the principal stress ratios k in Fig.-8. An average ratio of 0.99 and a coefficient of variation of 10.9% suggest applicability of the proposed formula.

4. Test Results of Laterally Loaded RCCV Models

In Fig.-9 skelton curves of horizontal load-displacement angle relationships are depicted for all the models including the four models previously reproted. The notation of the model such as C-1.8-3.0 indicates that the model had a reinforcement ratio of 1.8% in each direction and was subjected to sustained internal pressure of 3.0kg/cm^2. From the figure following general tendencies could be deduced.

(1) When the reinforcement ratio is constant, the lower the internal pressure, the larger

the horizontal load bearing capacity. The ductility, however, reduces as the internal pressure decreases. In particular, while the deformation angle of C-1.8-3.0 at the maximum load reached as high as 34×10^{-3} radian, that of C-1.8-0.0 was only 10×10^{-3} radian though the ultimate loads of the two models were practically the same.

(2) If the internal pressures are constant, the smaller the reinforcement ratio, the lower the ultimate strength. To the contrary the deformability increases with decrease in reinforcement ratio.

(3) Initial stiffnesses against lateral forces are reduced with decrease in reinforcement ratio and with increase in internal pressure.

(4) Shear deformations constitute 40∿60% of total horizontal deformations at the top slab of the models in post-diagonal-cracked stage.

As can be seen from Fig.-10 the loads at which the circumferential reinforcements yielded could be predicted up to the reinforcement ratios of 1.5% in terms of the effective shear reinforcement ratio proposed in the previous report [2]. The fact C-1.8-0.0 failed without accompanying any appreciable yielding in reinforcements suggests the importance of limiting the reinforcement ratio to an appropriate value when only an orthogonal reinforcement system is to be used.

The upper yielding load, which corresponds to yielding in reinforcements in the stronger direction (usually the vertical reinforcement) was calculated by the following equation, in which an averaged effective shear reinforcement ratio for the two directions is substituted in lieu of the value for the weaker direction.

$$\tau_y^{max} = \frac{1}{2} (P'_{w \cdot H} + P'_{w \cdot V}) \sigma_{sy} \qquad (5)$$

τ_y^{max} : upper shear yield stress at the web of RCCV.

$P'_{w \cdot H}$, $P'_{w \cdot V}$: effective shear reinforcement ratios for horizontal and vertical directions, respectively.

A good correlation was found between calculated and measured data by applying the above formula.

5. Conclusions

Following conclusions could be arrived at within the limit of the experiments.

(1) A satisfactory accuracy from the designer's oriented view point was obtained in predicting stresses in reinforcements, deformations as well as shear slips along a crack of orthogonally reinforced concrete shell elements by applying the proposed method, in which direction of cracks and shear rigidities across cracks are taken into account in conformity with experimental evidences.

(2) As were made clear in the tests of hollow cylindrical reinforced concrete models subjected to lateral forces the bearing capacities as well as the deformational behaviours are mainly governed by an interaction of reinforcement ratios and internal pressures. The engineering judgement of earthquake resistibility of a RCCV should be based on the requirements not only for strength, but for ductility as well.

Reference:

/1/ Y. AOYAGI, K. YAMADA "An Experimental Approach to the Design of Network Reinforcement Against In-plane Shear in Reinforced Concrete Containments" 5th SMiRT Conference Berlin, Germany (1979) J4/7

/2/ T. UCHIDA, N. OHMORI, T. TAKAHASHI, S. WATANABE, H. ABE, Y. AOYAGI "Behavior of Reinforced Concrete Containment Models under the Combined Action of Internal Pressure and Lateral Force" 5th SMiRT Conference Berlin, Germany (1979) J4/4

/3/ Th. Baumann "Tragwirkung orthogonaler Bewehrungsnetze beliebiger Richtung in Flächentragwerken aus Stahlbeton" Deutcher Ausschuss für Stahlbeton, Heft 217, Berlin 1972.

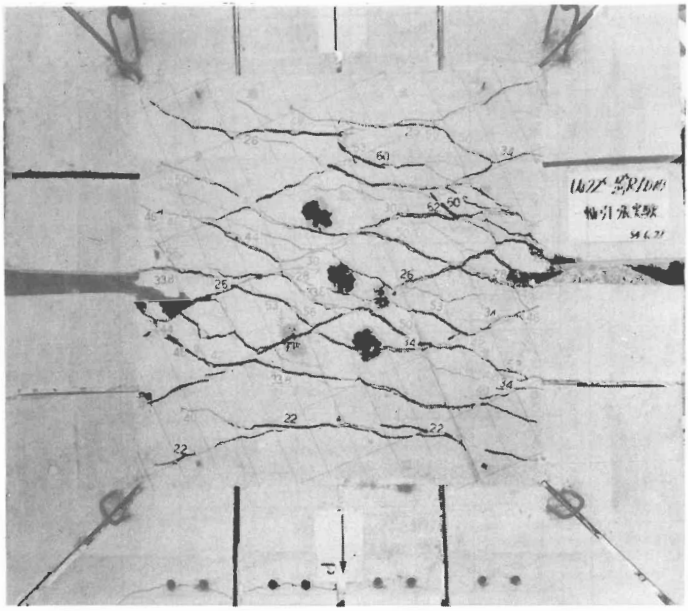

Fig.-1 Cracting Patterns of RC Shell Elements Models after Failure (NO24)

properties of specimens					strength data (ton)		
NO of spec.	reinforce-ment ratio(%)	inclination of reinfnce-ment.	initial crack	K= N_2/N_1	initial cracking load	yielding load	maximum load.
22	1.183	α = 0	None	0	30.0	—	92.0
23	1.183	22.5°	None	0	28.0	—	79.0
24	x : 1.183 y : 0.592	22.5°	None	0	22.0	58.5	65.0
25	1.183	22.5°	ϕ = 22.5°	0	—	—	82.5
26	1.183	45°	None	0	30.0	69.0	82.0
27	1.183	22.5°	None	0.5	26.0	64.0	87.5

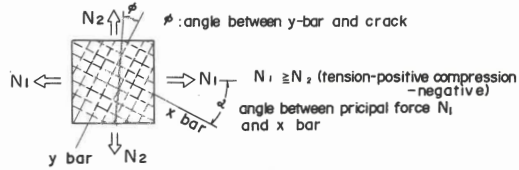

Table-1 Geometrical Properties and Strength Data of Plate Specimens

Notation of Models	C - 1.8 - 0.0	C - 3.0 - 3.0
mid-plane of diameter d (cm)	160	
wall thickness t (cm)	6	
height of cylinder h(cm)	160	
internal pressure p(kg/cm²)	0.0	3.0
reinforcement	H V a a D6 mm a = 59mm double	D6 mm a = 36mm double
flexural cracking load (ton)	10.0	cracks present prior to loading
flexural yield load (ton)	46.0	56.0
shear cracking load (ton)	20.7	30.0
shear yieding load for vert. reinf. (ton)	the same as the ultimate	98.9
shear yielding load for horiz. reinf. (ton)	〃	98.9
maxmum load	78.8	127.7
mode of failure	shear at midheight	shear at the junction between cylinder and base slab

Table-2 Dimensions and Main Test Results of Cylindrical Models

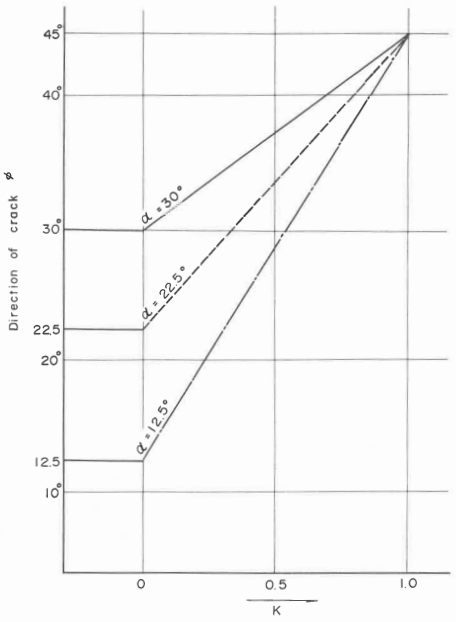

Fig.-2 Relationships between K and ϕ

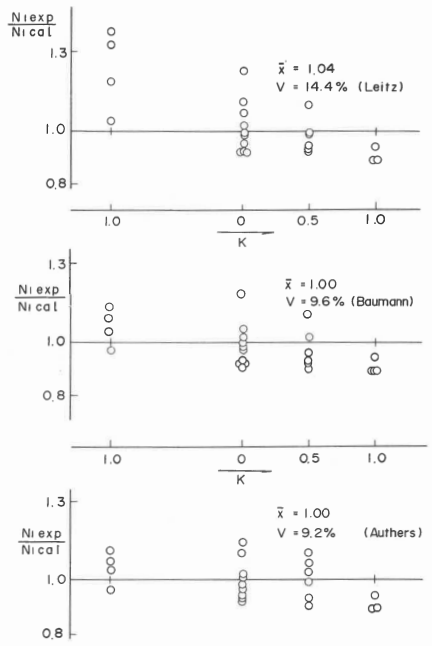

Fig.-5 Ratios of Calculated and Measured Loads causing Yield in x bars

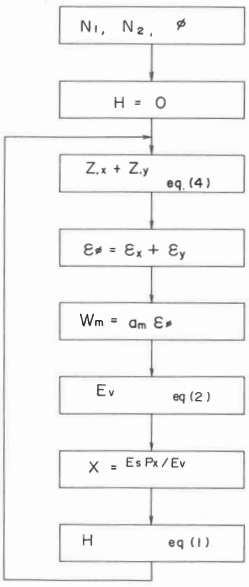

Fig.-3 Computation Flow for Determing H

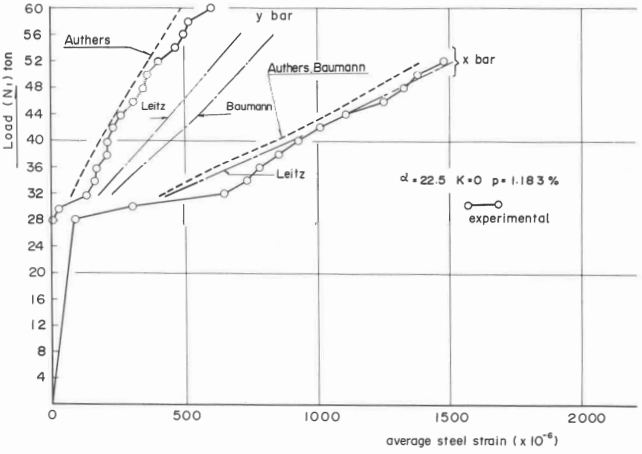

Fig.-4 Comparison of Measured Average Strains in Steels with Calculated

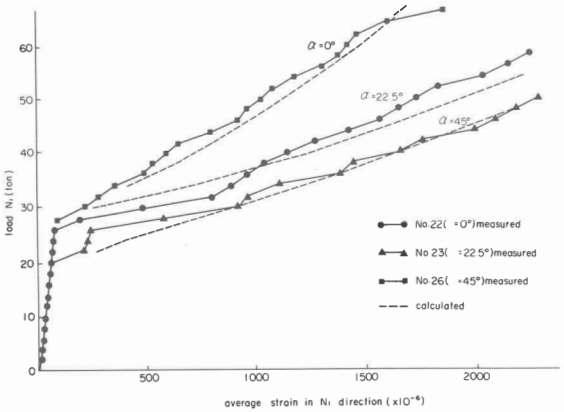

Fig.-6 Comparison of Measured Deformations in N_1 Direction with Calculated.

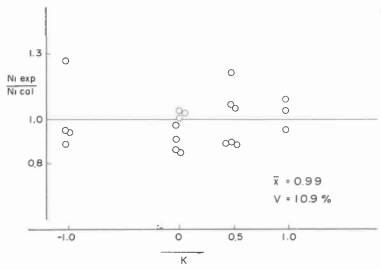

Fig.-8 Comparison of Measured Yielding Loads for y Reinforcement with Calculated

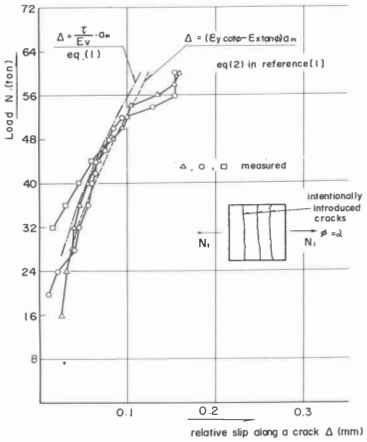

Fig.-7 Comparison of Measured Relative Slips along a Crack with Calculated

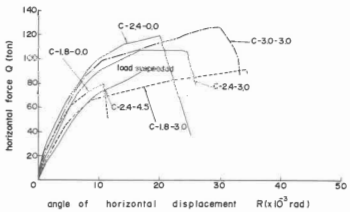

Fig.-9 Skelton Curves of Horizontal Load-Displacement Relationships for the Cylindrical Models

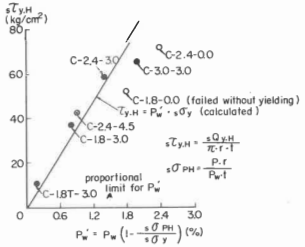

Fig.-10 Relationship between Effective Shear Reinforcement and Lower Shear Yielding Stress in RC Cylindrical Models

$_s\tau_{y\cdot H}$: Shear stress causing yield in hoop reinforcement

σ_{sy} : Yield point of steel

P_w : Web reinforcement ratio

P : Internal pressure

r : Internal radius